J Comput Aided Mol Des (2009) 23:261–272
DOI 10.1007/s10822-008-9256-x

Drug-resistant molecular mechanism of CRF01_AE HIV-1 protease due to V82F mutation

Xiaoqing Liu · Zhilong Xiu · Ce Hao

Received: 31 August 2008 / Accepted: 15 December 2008 / Published online: 15 February 2009

Abstract Human immunodeficiency virus type 1 protease (HIV-1 PR) is one of the major targets of anti-AIDS drug discovery. The circulating recombinant form 01 A/E (CRF01_AE, abbreviated AE) subtype is one of the most common HIV-1 subtypes, which is infecting more humans and is expanding rapidly throughout the world. It is, therefore, necessary to develop inhibitors against subtype AE HIV-1 PR. In this work, we have performed computer simulation of subtype AE HIV-1 PR with the drugs lopinavir (LPV) and nelfinavir (NFV), and examined the mechanism of resistance of the V82F mutation of this protease against LPV both structurally and energetically. The V82F mutation at the active site results in a conformational change of 79′s loop region and displacement of LPV from its proper binding site, and these changes lead to rotation of the side-chains of residues D25 and I50′. Consequently, the conformation of the binding cavity is deformed asymmetrically and some interactions between PR and LPV are destroyed. Additionally, by comparing the interactive mechanisms of LPV and NFV with HIV-1 PR we discovered that the presence of a dodecahydroisoquinoline ring at the P1′ subsite, a [2-(2,6-dimethylphenoxy)acetyl]amino group at the P2′ subsite, and an N2 atom at the P2 subsite could improve the binding affinity of the drug with AE HIV-1 PR. These findings are helpful for promising drug design.

Keywords CRF01_AE HIV-1 protease · Inhibitor · Resistance · Mutation · Molecular dynamics simulation

Electronic supplementary material The online version of this article (doi:10.1007/s10822-008-9256-x) contains supplementary material, which is available to authorized users.

X. Liu · Z. Xiu (✉)
Department of Bioscience and Biotechnology, School of Environmental and Biological Science and Technology, Dalian University of Technology, Dalian 116024, People's Republic of China
e-mail: zhlxiu@dlut.edu.cn

X. Liu
e-mail: lxq785348@163.com

C. Hao
Department of Chemistry, School of Chemical Science and Engineering, Dalian University of Technology, Dalian 116024, People's Republic of China

Introduction

One function of human immunodeficiency virus protease (HIV-PR) is to process gag and gag-pol polyprotein precursors, and this processing is essential for viral maturation [1–4]. Because inactivation of this enzyme will block viral assembly and infection, it is still one of the primary targets of anti-AIDS drug discovery [5–12]. There are two major types of HIV, one is type 1 (HIV-1), which is the most prevalent in the world, and the other is type 2 (HIV-2). HIV-1 contains three groups labeled M, N, and O. Viruses in group M are subdivided into subtypes, sub-subtypes, and circulating recombinant forms (CRFs) including A-D, A/E, A/G, F–H, J, and K forms [13]. In some developed regions (for example North America and Western Europe), subtype B(B) is responsible for the vast majority of HIV infections. Non-subtype B viruses are commonly found in the developing world.

HIV-1 PR consists of two identical 99-amino-acid monomers forming a homodimer with a central symmetric, substrate-binding cavity [14–16]. The catalytically active site located at the dimer interface is formed by the catalytic triad residues D25(25′)-T26(26′)-G27(27′), of which D25 and D25′ are known to be active residues. Many researchers have investigated the protonated states of aspartates D25 and D25′ and found that the states vary depending on the

binding ligands [17–19]. There is a flap region above the binding cavity; some researchers have reported that the flap closes on the active site upon substrate binding and opens for product release [20, 21].

Recently, eight antiviral agents (nelfinavir, saquinavir, indinavir, amprenavir, ritonavir, tipranavir, atazanavir, and lopinavir) have been approved by the Food and Drug Administration (FDA) for clinical use; others are still under clinical investigation [22]. These inhibitors bind to the substrate-binding cavity and have strong affinity for wild type B HIV-1 protease [23–26]. However the affinities of these inhibitors are highly affected by protease mutations. Some experimental and computational studies have revealed that some active site mutations changed the direct interactions between protease and inhibitor and caused unfavorable contact between them [27–40]. Some non-active site mutations, for example L10F, F53L, and L90M, have also been reported to indirectly change the interactions between protease and inhibitor, leading to reduced binding affinities between them [29, 32, 41–45]. Moreover, the currently available protease inhibitors are only active against the subtype B protease. There are few data demonstrating that these protease inhibitors have the same level of inhibition against different HIV-1 subtypes [46], and the question that the therapy for non-subtype B viruses may be less effective than for subtype B viruses has been raised owing to the residue polymorphisms in HIV-1 protease [47–50]. It is, therefore, necessary to design inhibitors against non-subtype B HIV-1 PR.

The circulating recombinant form 01 A/E (CRF01_AE, abbreviated AE) subtype, one of the most prevalent HIV-1 subtypes throughout the world, is predominantly found in Southeast Asia. The subtype AE is expanding rapidly and infecting a large number of people, especially in areas where the pandemic is uncontrolled [51–53]. It is, therefore, very important to understand the mechanism of interaction of subtype AE HIV-1 PR with its inhibitors, and develop drugs against AE HIV-1 protease.

The V82F mutation often occurs in HIV-1 PR and is highly resistant to some inhibitors [54, 55]. Lopinavir (LPV) and nelfinavir (NFV) are two kinds of AE HIV-1 PR inhibitor. The structure of AE HIV-1 protease and the chemical structures of LPV and NFV are shown in Fig. 1. LPV loses its ability to inhibit the AE HIV-1 PR which has the V82F mutation, whereas the V82F mutation has little influence on the inhibition ability of NFV [56]. In addition, the binding affinity of LPV with the subtype AE HIV-1 PR is higher than that of NFV with this PR, even if the V82F mutation occurs in the complex of AE HIV-1 PR and LPV. Hence, in this work, we performed molecular dynamics simulations of subtype AE HIV-1 PR complexed with LPV and NFV ligands to clarify the molecular mechanism of resistance against LPV because of the V82F mutation.

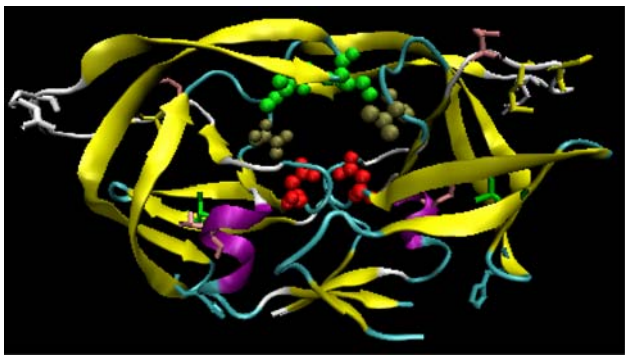

(a)

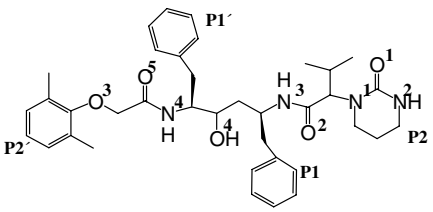

(b)

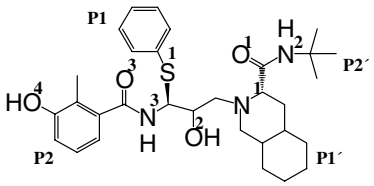

(c)

```
                10        20        30        40
B:  PQITLWQRPLVTIKIGGQLKEALLDTGADDTVLEEMSLPGRWKPKMIGG

AE: PQITLWQRPLVTVKIGGQLKEALLDTGADDTVLEDINLPGKWKPKMIGG

    50        60        70        80        90        99
B:  IGGFIKVRQYDQILIEICGHKAIGTVLVGPTPVNIIGRNLLTQIGCTLNF

AE: IGGFIKVRQYDQILIEICGKKAIGTVLVGPTPVNIIGRNMLTQIGCTLNF
```

(d)

Fig. 1 (**a**) Structure of the subtype AE HIV-1 protease used in this study. Locations of two catalytic aspartates (*red*), the 50th residues (*blue*), and the 82nd residues (*brown*), are shown in Corey–Pauling–Koltun (CPK) representation. Locations of polymorphisms in subtype AE protease (I13 V, E35D, M36I, S37 N, R41 K, H69 K, and L89 M) are shown in stick representation. (**b**) and (**c**) are chemical structures of LPV and NFV, respectively. Only the atoms of N, O, and S are labeled. (**d**) Amino acid sequence of subtype B HIV-1 protease and subtype AE HIV-1 protease. The polymorphisms in subtype AE protease is highlighted in *red letters*

Some obvious differences, for example the conformational change of the 79′s loop region, the rotation of the side-chains of residues D25 and I50′, and the structural change of the binding cavity, can be seen by comparing the complexes of LPV and wild-type and V82F mutant AE HIV-1 PR. Our work will be useful in the design of better inhibitors which

not only have high binding affinity for the subtype AE HIV-1 PR but also have little effect on the V82F mutation.

Materials and methods

Preparation of starting structures

The initial structures for the subtype AE HIV-1 protease in complexes with LPV and NFV were modeled from the X-ray crystal structures of subtype B HIV-1 protease complexed with the two inhibitors (PDB code: 1MUI [57] and 1OHR [58], respectively) using the LEaP module in the Amber 9.0 package [59]. The V82F complexes were also constructed using the two crystal structures as models. All missing atoms and hydrogen atoms of the complexes were also added using the LEaP module.

The atom charges for protease inhibitors utilized in the MD simulations were generated using quantum chemical methods. Geometry optimization and the electrostatic potential were calculated for each protease inhibitor at the B3LYP/6-31G(d) level of theory using Gaussian03 program [60]. The partial atom charges of the inhibitors were obtained by the RESP method [61]. Force-field data for protease inhibitors were generated by means of the Antechamber module of Amber 9.0. The Amber ff99 force field [62] was used for the van der Waals and bonded energy terms. The protonation states of catalytic aspartate residues D25 and D25′ in the active site vary depending on the binding inhibitors or substrates. According to the PK_a calculation, in this work, one of the two aspartyl residues D25/D25′ was protonated and the other was deprotonated for the four complexes, which was computed by PDB2PQR Server [63].

Each complex was inserted in a cubic box filled with TIP3P water molecules. The crystal water molecules were conserved in each system. In order to neutralize the system, chlorine ions were added in the system using the LEaP module.

Molecular dynamics simulations

Minimization and molecular dynamics simulations were carried out with the Sander module of Amber 9.0. The minimization was performed in four steps, the first three steps kept the solute fixed with forces of 500 kcal/(mol Å^2), 300 kcal/(mol Å^2), and 100 kcal/(mol Å^2), respectively, and the last minimization was applied to the whole systems without any force. Two-thousand five-hundred steps of the steepest descents and 2,500 steps of the conjugate gradients were used for every step. The whole systems were then slowly heated from 0 K to 300 K over 60 ps with a force constant of 10 kcal/(mol Å^2) for the solutes. Subsequently, the systems were equilibrated in the NVT ensemble and in the isobaric–isothermal (NPT) ensemble, respectively, for 100 ps and a force of 10 kcal/(mol Å^2) was used for the solutes in the two ensembles. Last, the whole systems were equilibrated in the NPT ensemble for 50 ps without any force. The MD simulation was carried out employing the periodic boundary condition with the NPT ensemble for 1.2 ns. The SHAKE algorithm [64] was used to constrain all atoms involving hydrogen atoms, and the time step was set to 2 fs. The atom coordinates were collected every 1 ps. The partial mesh Ewald (PME) method [65] was employed to treat long-range electrostatic interactions. The MD simulations showed no large fluctuations for the last 400 ps simulation (the data are shown in Supporting Information Fig. S1.). Hence, coordinates of 400 snapshots for the last 400 ps were obtained to analyze the structure in detail.

Binding energy calculation

The binding free energy was calculated using MM/PBSA methodology [66] according to the equation:

$$\Delta G = \Delta G_{\mathrm{MM}} + \Delta G_{\mathrm{sol}} - -T\Delta S$$

where ΔG is the binding free energy in solution, ΔG_{MM} is the molecular mechanics free energy, ΔG_{sol} is the solvation free energy, and $-T\Delta S$ represents the contribution of entropy to the binding energy. ΔG_{MM} and ΔG_{sol} were defined by the equations:

$$\Delta G_{\mathrm{MM}} = \Delta G_{\mathrm{vdw}} + \Delta G_{\mathrm{ele}},$$

$$\Delta G_{\mathrm{sol}} = \Delta G_{\mathrm{pol,sol}} + \Delta G_{\mathrm{nonpol,sol}}$$

where ΔG_{vdw}, ΔG_{ele}, $\Delta G_{\mathrm{pol,sol}}$, and $\Delta G_{\mathrm{nonpol,sol}}$ are the van der Waals interaction energy, the electrostatic interaction energy, the polar contribution to solvation, and the hydrophobic contribution to solvation, respectively. ΔG_{vdw} and ΔG_{ele} were computed using the Sander program of Amber 9.0. The polar solvation contribution was calculated by solving the Poisson–Boltzmann equation implemented in the Delphi program [67]. The dielectric constants of solute and water were set to 2.0 and 80.0, respectively. The hydrophobic contribution term was computed as:

$$\Delta G_{\mathrm{nonpol,sol}} = \gamma A + b$$

where A represents the solvent-accessible surface area, and the solvation parameters γ and b were set to 0.00542 kcal/(mol Å^2) and 0.92 kcal/mol [68], respectively. The conformational entropy was estimated using the *nmode* program in Amber 9.0 [59]. Ten snapshots were collected at intervals of 40 ps for the last 400 ps to analyze the

contribution of entropy. The molecular mechanics free energy (ΔG_{MM}) and the solvation free energy (ΔG_{sol}) were calculated for 200 snapshots during the last 400 ps (extracting one snapshot every 2 ps).

Root mean square deviation (RMSD)

The root mean square deviation (RMSD) is a numerical measure of the difference between two structures. The formula for the RMSD for every residue between the average structure of AE PR and that of V82F PR was given by:

$$\mathrm{RMSD} = \sqrt{\sum_{i\in\{N,C\alpha,C\}} \frac{\left((\vec{r}_i(AE) - \langle\vec{r}_i\rangle)^2 + (\vec{r}_i(V82F) - \langle\vec{r}_i\rangle)^2\right)}{198}}$$

where $\vec{r}_i$ is the position of atom i in every residue of each average structure, which took the coordinate of the first time step of the respective simulation as a reference. $\langle\vec{r}_i\rangle$ is the average position of atom i in the two average structures, which was defined as:

$$\langle\vec{r}_i\rangle = \frac{\vec{r}_i(AE) + \vec{r}_i(V82F)}{2}, \quad i \in \{N, C\alpha, C\}.$$

Buried surface area (SA)

The solvate-accessible surface area (SA) was computed for ligand only, for free protease, and for ligand-bound protease. The buried SA was calculated as follows:

$$\mathrm{Buried\,SA} = \mathrm{SA_{ligand}} + \mathrm{SA_{free-protease}} - \mathrm{SA_{ligand-boundprotease}}.$$

The SA [69] was computed with Paul Beroza's molsurf program developed by Connolly [70].

Results

Binding energy calculation

The binding free energy was calculated by use of the MM/PBSA method. The results for all the models are shown in Table 1. It is clear that the simulation results within the standard deviation are consistent with the experimental results. V82F has almost the same affinity as AE protease for NFV. On the other hand, V82F greatly reduces the binding free energy of LPV. Additionally, irrespective of whether or not the V82F mutation occurs, the binding affinities of LPV with AE HIV-1 PR are higher than those of NFV with this protease. Hence, the effect of V82F mutation on binding free energy was examined structurally for each complex.

Structure comparison between WT and V82F

In order to examine the effect of the V82F mutation on the active site conformations, the average structures of the V82F models are compared with those of the corresponding AE models for the last 400 ps. The RMSD values between the average structures of the V82F models and those of the AE models were calculated according to the coordinates of the main-chain atoms N, C, and Cα (Table 2). In this work we only compare the residues in the active cavity. In the case of the LPV model, the main-chain atoms in the flap region (residues I47/I47′, G48/G48′, G49/G49′, and I50/I50′) and those in the 79′s loop region (residues P79/P79′, T80/T80′, P81/P81′, V82/V82′, N83/N83′, and I84/I84′) show large differences. For the NFV model, the main atoms in the two regions also exhibit large deviation. However the RMSD values for the two regions in the NFV model are smaller than those in the LPV model.

Table 1 Binding energy of each compound (kcal/mol)

		ΔG_{vdw}	ΔG_{elec}	$\Delta G_{pol,sol}$	$\Delta G_{nonpol,sol}$	ΔG_b^a	-TΔS	ΔG_b^b	$\Delta\Delta G_b^c$	$\Delta\Delta G^d$
NFV	AE	−64.90	−15.19	44.32	−7.60	−43.37	26.21	−17.16	−0.01	0.36
		(3.74)	(2.07)	(2.76)	(0.18)	(3.28)	(10.40)	(7.71)		
	V82F	−67.16	−18.17	48.33	−7.62	−44.61	27.44	−17.17		
		(3.06)	(4.51)	(3.66)	(0.09)	(3.22)	(4.97)	(4.19)		
LPV	AE	−75.33	−24.67	48.43	−8.23	−59.80	26.18	−33.62	15.24	1.93
		(3.45)	(2.78)	(2.54)	(0.14)	(3.28)	(5.07)	(4.27)		
	V82F	−72.89	−21.00	50.54	−8.04	−51.39	33.01	−18.38		
		(3.35)	(2.63)	(2.83)	(0.11)	(3.94)	(4.55)	(4.26)		

[a] The predictions do not include entropy effect

[b] The predictions include entropy effect

[c] Difference from AE, i.e., $\Delta\Delta G = \Delta G_{V82F} - \Delta G_{AE}$

[d] Results from Ref. [56]; the calculation of binding energy is according to the formula $\Delta G = RT\ln K_i$, R = 8.314 and T = 300 K

[e] The values in parentheses are the standard deviations

Table 2 RMSD value (Å) of the residues in the active site between the AE and V82F models

Residues	LPV	NFV	Residues	LPV	NFV
L23	0.87 ± 0.56	0.64 ± 0.54	L23′	0.94 ± 0.52	0.67±0.57
L24	0.73 ± 0.57	0.53 ± 0.58	L24′	0.75±0.55	0.55±0.58
D25	0.42 ± 0.51	0.36 ± 0.67	D25′	0.48 ± 0.55	0.33 ± 0.53
T26	0.34 ± 0.54	0.30 ± 0.68	T26′	0.44 ± 0.61	0.25 ± 0.58
G27	0.19 ± 0.57	0.13 ± 0.70	G27′	0.29 ± 0.65	0.10 ± 0.64
A28	0.18 ± 0.54	0.16 ± 0.74	A28′	0.15 ± 0.57	0.22 ± 0.62
D29	0.31 ± 0.52	0.33 ± 0.69	D29′	0.27 ± 0.59	0.36 ± 0.71
D30	0.45 ± 0.55	0.55 ± 0.63	D30′	0.28 ± 0.56	0.59 ± 0.67
T31	0.67 ± 0.48	0.76 ± 0.52	T31′	0.57 ± 0.48	0.79 ± 0.57
V32	0.96 ± 0.49	0.84 ± 0.53	V32′	0.82 ± 0.49	0.91 ± 0.50
I47	**1.45 ± 0.72**	**0.77 ± 0.87**	I47′	**0.85 ± 0.75**	**1.11 ± 0.73**
G48	**1.29 ± 0.76**	**0.69 ± 0.85**	G48′	**0.87 ± 0.75**	**0.94 ± 0.76**
G49	**1.14 ± 0.78**	**0.70 ± 0.95**	G49′	**0.85 ± 0.77**	**0.83 ± 0.77**
I50	**0.90 ± 0.70**	**0.84 ± 0.92**	I50′	**1.15 ± 0.85**	**0.83 ± 0.81**
P79	**1.74 ± 0.88**	**1.28 ± 0.79**	P79′	**1.50 ± 0.94**	**1.21 ± 0.89**
T80	**1.47 ± 0.78**	**1.08 ± 0.69**	T80′	**1.35 ± 0.86**	**0.96 ± 0.90**
P81	**1.38 ± 0.81**	**1.02 ± 0.72**	P81′	**1.44 ± 0.92**	**0.75 ± 0.95**
V82	**1.21 ± 0.72**	**0.90 ± 0.67**	V82′	**1.27 ± 0.73**	**0.75 ± 0.77**
N83	1.11 ± 0.53	0.87 ± 0.53	N83′	1.15 ± 0.53	**0.84 ± 0.61**
I84	0.81 ± 0.48	0.69 ± 0.49	I84′	0.83 ± 0.48	0.73 ± 0.51

Error σ is calculated from $\sigma = [\sigma(\mathrm{WT})^2 + \sigma(\mathrm{V82F})^2]^{1/2}$, where σ(WT) and σ(V82F) are RMSF (Å) values of the main chain atoms N, C, and Cα of each residue. The values of RMSD ≥0.7 and $\sigma \geq 0.6$ are shown in bold

Similar results can be found regarding the residues at the flap region [71]. The reason is that these residues are very flexible (Supporting Information Fig. S2). The extent of the flap change is simply characterized by the distances of I50-Cα/D25-Cβ (chain A) and of I50′-Cα/D25′-Cβ (chain B). Measurement of the I50–D25 distance or the I50′–D25′ distance is more reasonable than measurement of the tip–tip (I50–I50′) distance, because the tip–tip distance can be affected by both flap tip curling and flap asymmetry. The distributions of these distances are shown in Fig. 2. The *T*-test was used to show how different the two distributions are in each graph. At the 0.05 level, we suppose the difference of the population means in each graph is greater than 0.3 Å, and the *p* values in Fig. 2 are as follows: (a) 0.005, (b) 0, (c) 0.704, and (d) 0.362. These data suggest that the difference between the two distributions in graphs (a) and (b) are larger than those in graphs (c) and (d), i.e. the active site conformation is more stable in the NFV model than that in the LPV model for the V82F mutation. The average structure of each ligand in the WT and V82F models is also compared Fig. 3). The P1, P1′, P2, and P2′ subsites of the LPV model are found to exhibit large deviation, and the atoms O2 and O4 of this ligand are also dislocated to quite different positions. For the NFV model, however, all the subsites have almost identical conformations. These structural changes in LPV model lead to the disappearance of some interactions between LPV and protease, for example hydrogen bonds and hydrophobic interactions.

Hydrogen bonds between PR and ligands

It is well known that hydrogen bonds play an important role in the combination of proteins with ligands. The formation of a hydrogen bond is defined using the following criteria:

1 the distance between donor and acceptor heavy atom is ≤3.5 Å; and

2 the donor-H–acceptor angle is ≥120°.

The 400 snapshots during the last 400 ps were extracted to analyze the direct or water-mediated hydrogen bonds. Figure 4 shows the hydrogen bonds between the protease and each ligand. There are mainly four direct hydrogen bonds between LPV and AE PR. They are from the side-chain of residue D29 (29OD1) to atom N2 of LPV (199N2), from the side-chain of residue D25′ (25′OD2/25′OD1) to atom N4 (199N4) and the central hydroxyl oxygen of LPV (199O4), and from the backbone N atom of residue I50 (50 N) to atom O2 of LPV (199O2). However in the complex of V82F PR and LPV, the hydrogen bonds 25′OD2–199N4 and 50 N–199O2 disappear. The disappearance of

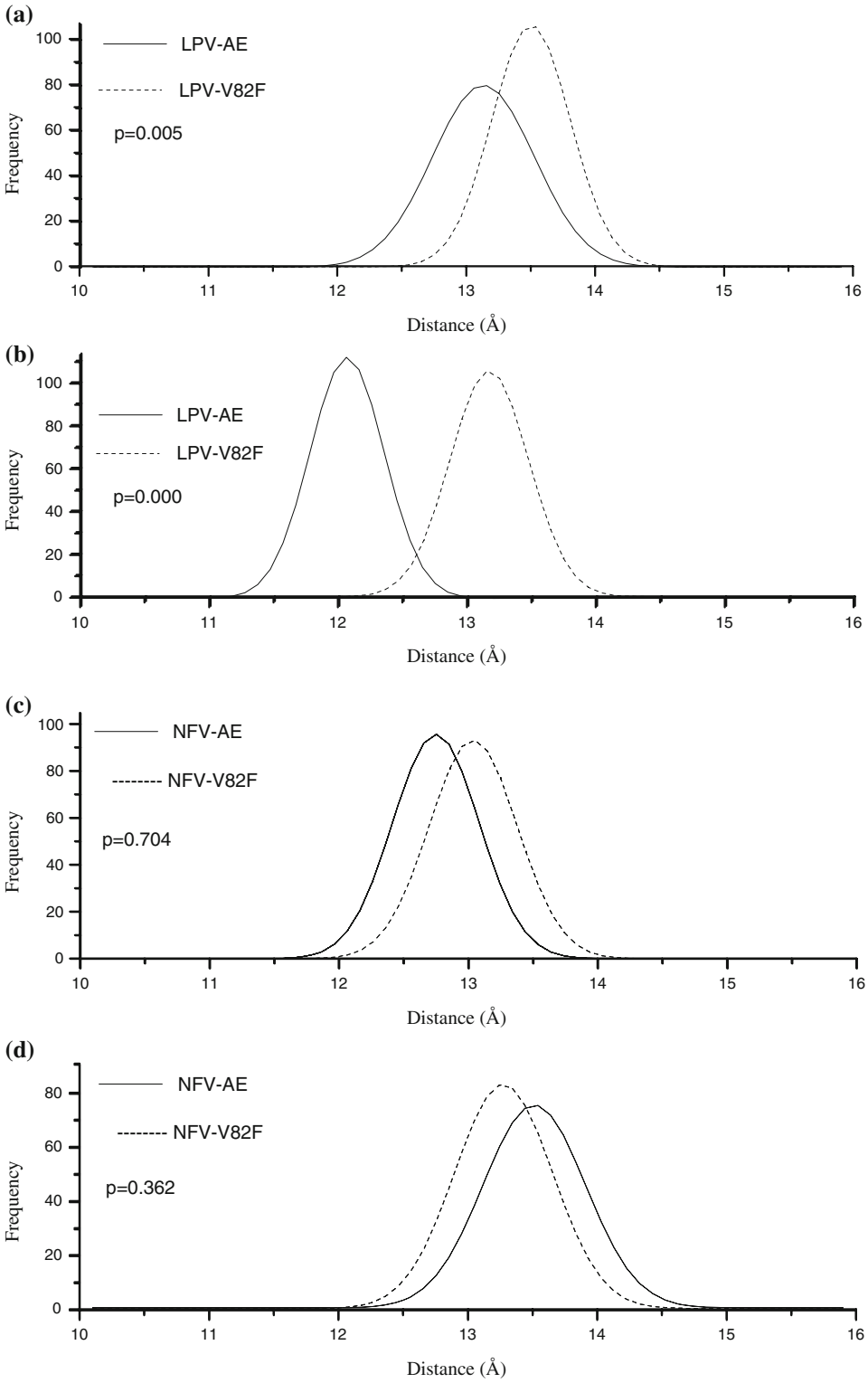

Fig. 2 Distributions of the Cα-Ile50′/Cβ-Asp25′ (**a**), the Cα-Ile50/Cβ-Asp25 (**b**) in LPV complexes, the Cα-Ile50′/Cβ-Asp25′ (**c**) and the Cα-Ile50/Cβ-Asp25 (**d**) in NFV complexes. μ represents the average value of gaussian distribution. The p values from the t-tests are also listed

the two hydrogen bonds greatly reduces the free energy contributions of residues I50 and D25′ (Fig. 5), although one water molecule links the side-chain of D25′ (25′OD1) with atom N3 of LPV (199N3). In the AE–LPV complex, there is only one water-mediated hydrogen bond between 27O and 199N3. Similar hydrogen bonds exist in the AE–NFV and V82F–NFV complexes, as follows:

1 the central hydroxyl oxygen of NFV (199O2) creates one direct hydrogen bond with the side-chain of D25′ (25′OD2);

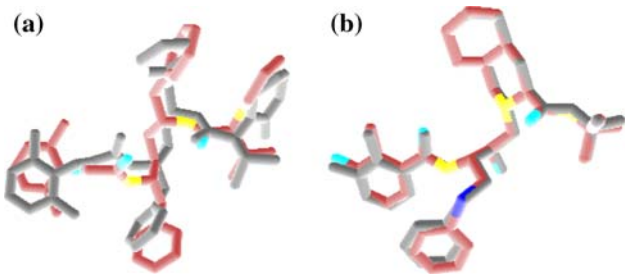

Fig. 3 Comparison of the structures of each ligand in the AE (*gray*) and V82F (*color*) models, (**a**) LPV ligand, (**b**) NFV ligand

2 water molecule 209 mediates the interaction between the backbone atom N of I50′ (50′N) and atom O1 of NFV (199O1).

Water molecule 219 also creates one hydrogen bond between the backbone atom N of D29′ (29′N) and atom N2 of NFV (199N2).

Hydrophobic interactions between the PR and ligands

It can be seen from Table 1 that the van der Waals interactions contribute the most to stabilizing the complex. The SA buried by the complexation is examined, which is in relation to the hydrophobicity of the binding cavity and the magnitude of van der Waals contacts between the ligand and PR [72–74]. Figure 6 shows the buried SA of most residues in the active cavity. In the LPV model, the buried

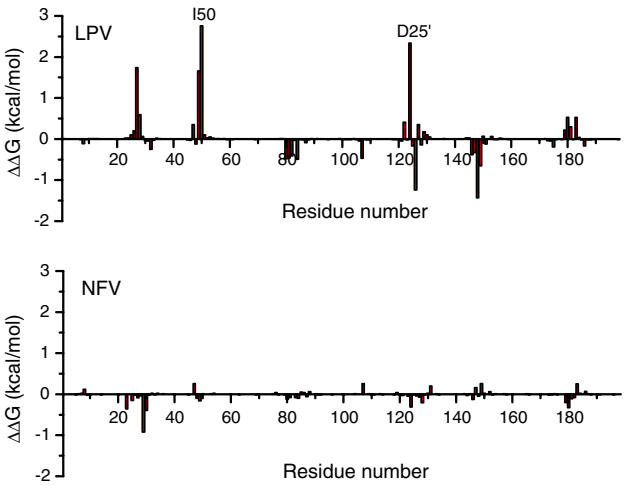

Fig. 5 The electronic energy difference between the inhibitor–residue interactions of the AE PR–ligand complex and those of V82F PR–ligand complex. $\Delta\Delta G = \Delta G_{V82F} - \Delta G_{AE}$. A positive value indicates the residue is favorable for the combination of AE PR and ligand

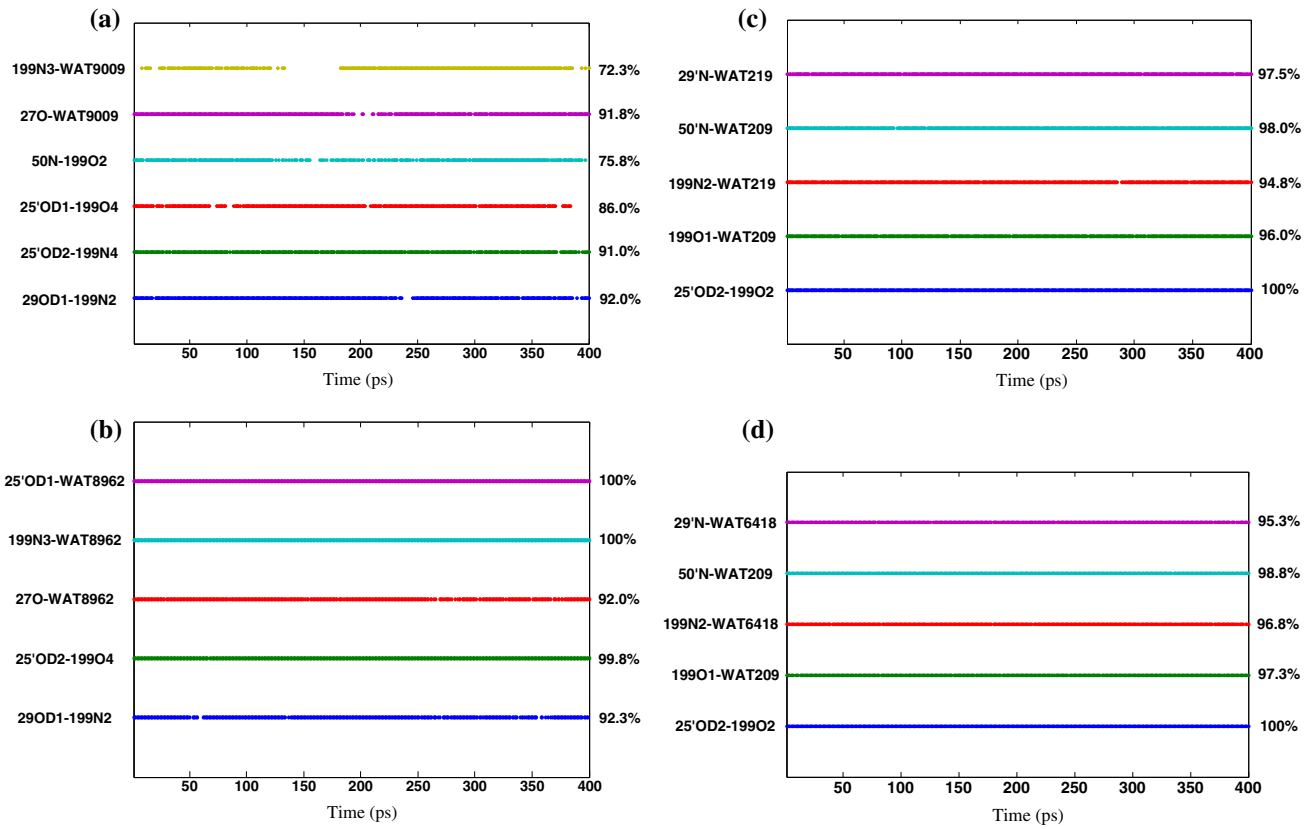

Fig. 4 Direct or one-water-mediated hydrogen bond networks during the last 400 ps in models LPV-AE (**a**), LPV-V82F (**b**), NFV-AE (**c**) and NFV-V82F (**d**). 199 represents LPV or NFV. The formation of a hydrogen bond was defined by use of the criteria given above

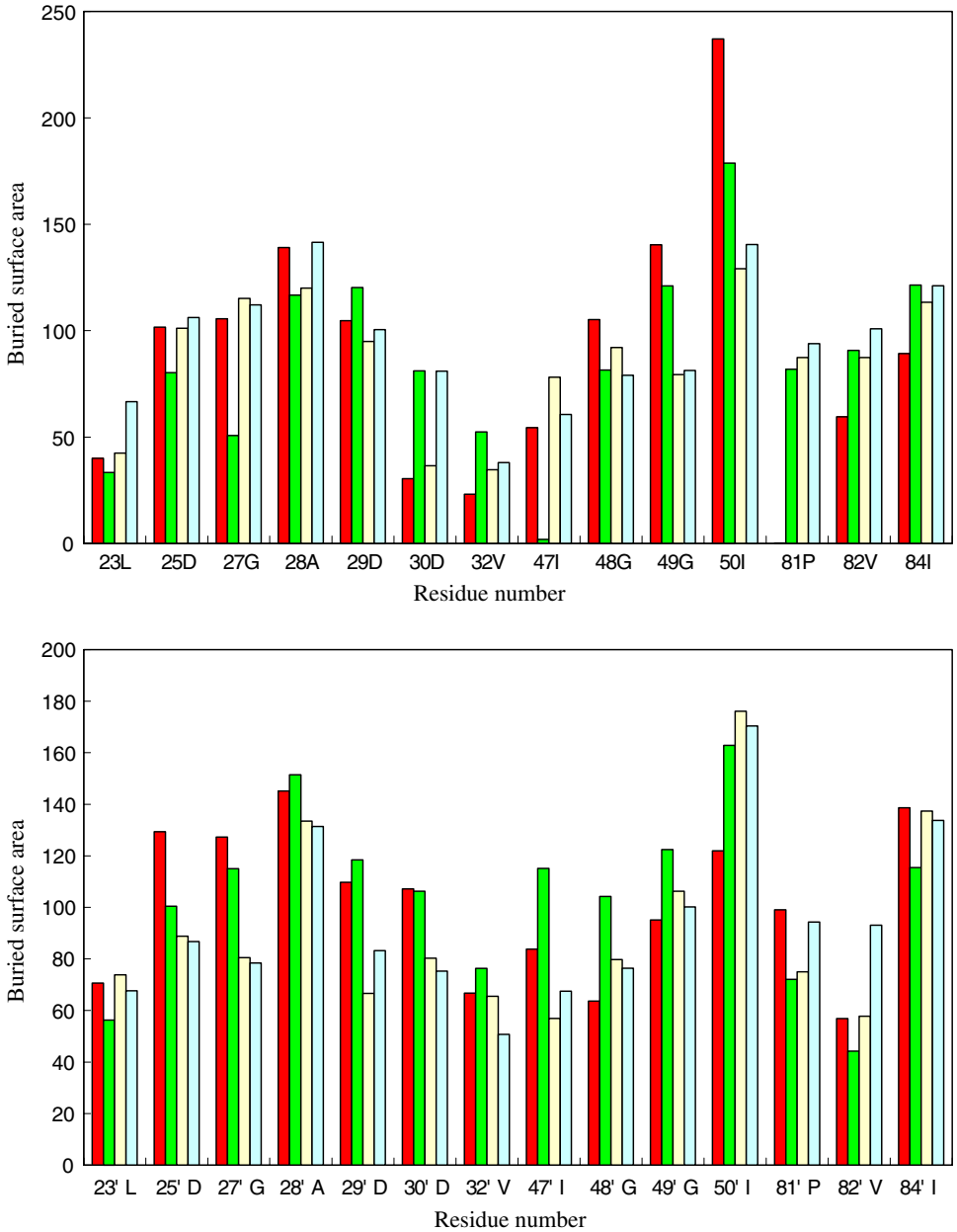

Fig. 6 Buried SAs of most residues in the active cavity. The *upper graph* represents those of chain A, and the *lower graph* represents those of chain B. The *red column*, *green column*, *yellow column*, and *blue column* represent LPV-AE, LPV-V82F, NFV-AE, and NFV-V82F, respectively

SAs of residues I50, P81′, V82′, I84′, and D25′ in V82F PR are smaller than those in AE PR, especially residue I50, whereas the buried SAs of residues I50′, P81, V82, and I84 are larger in V82F PR than those in AE PR. The buried SAs of these residues show little change between AE PR and V82F PR in the NFV model.

Molecular mechanism of conformational changes at the active site

It is obvious that residues P81–I84 are in close contact with the I50′, D25, and P1 subsites of each ligand, and residues P81′–I84′ are in close touch with the I50, D25′, and P1′ subsites of each ligand (Fig. 7). The residues P81–I84 and I50 are hydrophobic residues [31]. Hence, there are strong hydrophobic interactions between these and the P1/P1′ subsites of the ligand. Furthermore, the residues D25/D25′ are important residues for the HIV-1 PR; they create rigid hydrogen bond networks, i.e., fireman grips [75], and should have the least fluctuation. So, to examine the reason for these conformational changes at the active site induced by the mutation of V82F, we should pay attention to these residues. We find the side-chains of residues I50′ and D25 have large conformational changes in the LPV model (Fig. 8), which induce changes of the distances of Cα-Ile50/Cβ-Asp25 and of Cα-Ile50′/Cβ-Asp25′ (Fig. 3). As a result, the conformation of the active cavity is deformed asymmetrically, and some interactions between the ligand

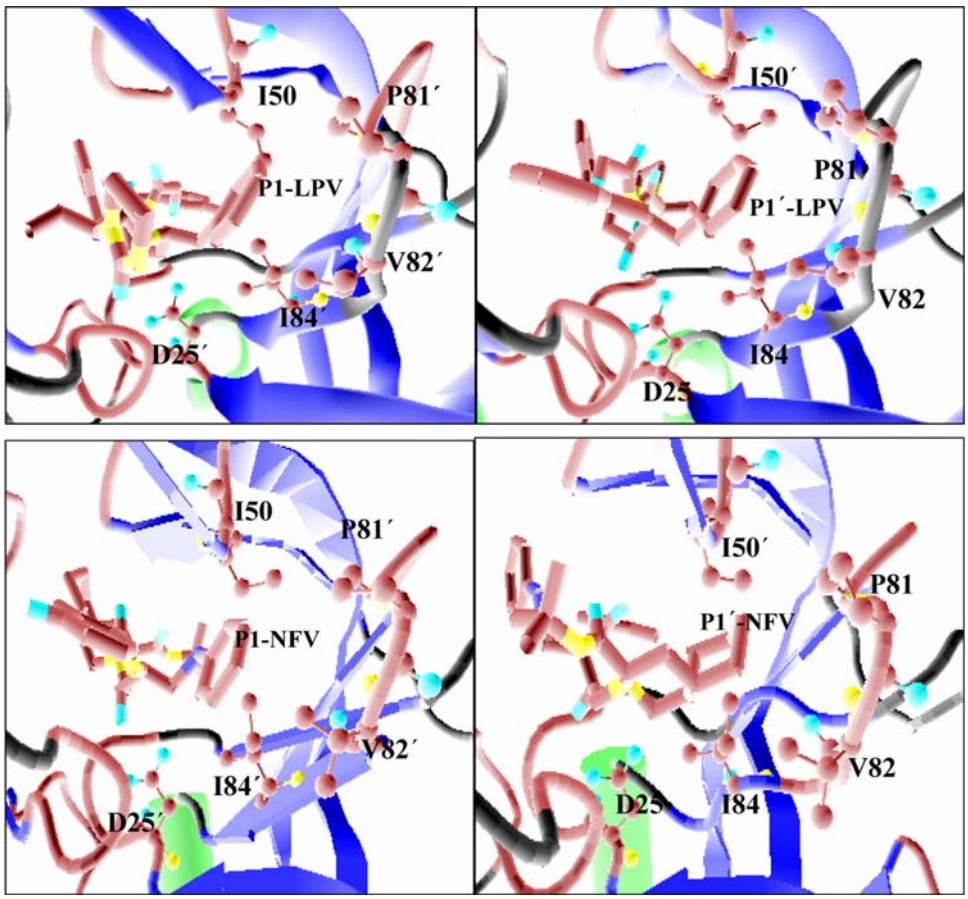

Fig. 7 The structures around the P1 and P1′ subsites of each ligand. The *colored sections* represent the structure of the PR. The ligands and important residues are shown in *bond* and *ball-and-stick* representations, respectively

and the residues in the active cavity are changed. These interactions are as follows:

- first, the conformational changes of the 79′s loop region make the P1 subsite of LPV dislocate, consequently, the van der Waals energy between the ligand and residue I50 are substantially reduced (Supporting Information Fig. S3);
- second, the displacements of atoms O2 and N4 of LPV lead to the disappearance of the hydrogen bonds 50 N–199O2 and 25′OD2–199N4, and the electronic energy contributions of D25′ and I50 are decreased, especially for the residue D25′ (Supporting Information Fig. S4).

So we speculate the mechanism of the active cavity conformational change is as follows:

- first, the V82F mutation changes the conformation of 79′s loop region;
- second, the side-chains of I50′ and D25 are rotated;
- third, the changes of the distances of Cα-Ile50/Cβ-Asp25 and of Cα-Ile50′/Cβ-Asp25′ cause conformational distortion of the active cavity; and
- finally, the displacements of some atoms in LPV destroy some interactions between the ligand and PR.

Discussion

In this study we performed MD simulations for the purpose of clarifying:

1 the mechanism of molecular resistance against LPV of the active site mutation V82F in subtype AE HIV-1 PR;
2 the reason the affinity of LPV for HIV-1 PR is higher than that of NFV for this protease; and
3 guidelines for the design of better drugs.

The V82F mutation hardly influences the affinity of NFV with PR, so the structures of LPV in the complex with this protease were analyzed in detail.

In the LPV model, the V82F mutation induces a conformational change of the 79′s loop region. The side-chain of residue I50′ rotates owing to its close contact with the 79′s loop region. The side-chain of residue D25 is also displaced. These side-chain conformational changes make the conformation of the active cavity deform asymmetrically. The V82F mutation also dislocates the positions of some atoms of LPV, and reduces some interactions between this ligand and some residues in the active cavity. So the affinity of LPV for PR because of the V82F mutation is reduced seriously. Although the conformations of

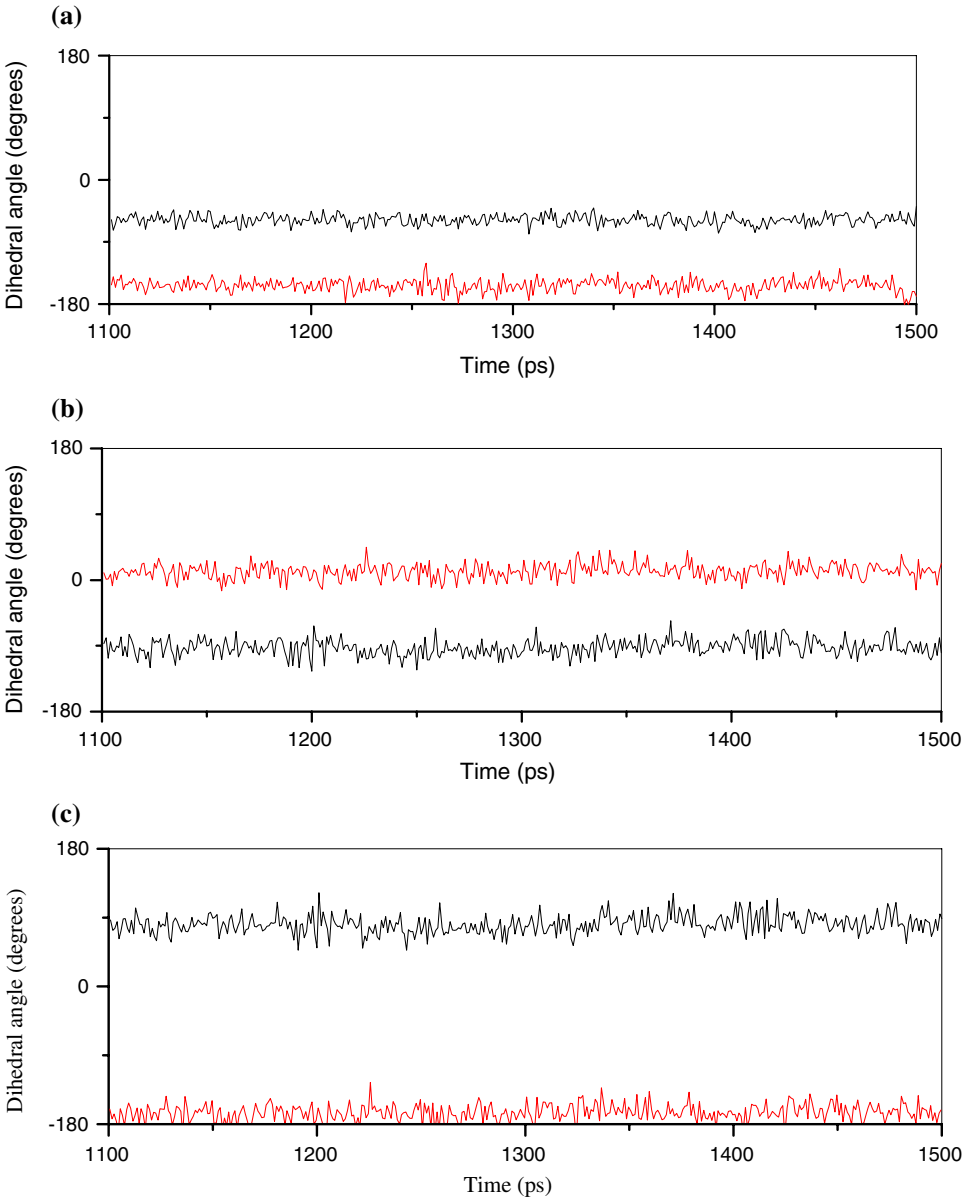

Fig. 8 Trajectory of dihedral angles of N-Cα-Cβ-Cγ1 of I50′ (**a**), of Cα-Cβ-Cγ-Cδ1 of D25 (**b**), and of Cα-Cβ-Cγ-Cδ2 of D25 (**c**). *Black lines* represent the LPV-AE model and *red lines* represent the LPV-V82F model

the 79′s loop region also have some changes in the NFV model, these changes are smaller than those in the LPV model. The side-chains of I50/I50′ and D25/D25′ do not change (Supporting Information Fig. S5). Therefore the structure of the active cavity is almost identical. In addition, NFV superimposes very well between the AE model and the V82F model, and the interactions between NFV and PR are nearly the same also (Fig. 3), which lead to similarities of the free energy contribution of every residue (Fig. 5). Hence, the V82F mutation has little influence on the NFV complex. However, another question of why the rotations of the side-chains of I50′ and D25 occur in V82F-LPV complex but do not occur in V82F-NFV complex still need to be answered. This is because the rotations result from not only the change of the 79′s loop region but also from the geometry of the ligand. Observing the P1′ subsites of the two ligands, we find NFV contains a dodecahydroisoquinoline ring, which is a bulky and rigid functional group, and LPV contains a phenyl ring. Both rings are near residues D25 and I50′. The dislocation of the phenyl ring because of the V82F mutation results in an unfavorable collision of the side-chains of I50′ and D25, and results in their rotation in LPV complexes (Supporting Information Fig. S6.). In contrast, the dodecahydroisoquinoline ring is relatively steady in the V82F mutation because of its large volume. Therefore the size of the rings at the P1′ subsite is responsible for the resistance of the V82F mutation.

Another important phenomenon that should be noted is that the affinity of LPV for AE/V82F PR is higher than that of NFV for AE/V82F PR. From Table 1 it can be seen that the electronic energies and van der Waals energies in LPV complexes are higher than those in NFV complexes. We

analyze two aspects of these complexes. First, because hydrogen bonds are one of the important factors contributing to the electronic energy, we investigated their hydrogen bonds and found that there are at least two hydrogen bonds in LPV complexes. One is between the side-chain of residue D25′ and the hydroxyl oxygen of LPV, and the other is 29OD1–199N2. In NFV complexes, however, there is only one hydrogen bond 25′OD2–199O2. Hence, the existence of hydrogen bond 29OD1–199N2 is very important for binding of the ligand with the PR. Second, we compared the P2′ subsites of the two ligands, which is a [2-(2,6-dimethylphenoxy)acetyl]amino group in LPV and a *tert*-butylcarboxamide group in NFV. The two subsites locate in the S2′ pockets comprised of residues D29′, D30′, and I47′ of the PR (Supporting Information Fig. S7). The buried surface areas of these residues with the LPV are larger than those with the NFV (Fig. 6), so the van der Waals energies of these residues in LPV complexes are higher than those in NFV complexes (Table S1). However, the van der Waals energies of residues I50′ and P81 in the S1′ pocket are higher in NFV complexes than those in LPV complexes, because the buried surface areas of the dodecahydroisoquinoline ring of NFV with the two residues are larger than those of the phenyl ring of LPV with these residues (Fig. 6). On the basis of this analysis, it can be concluded that the hydrogen bond 29OD1–199N2, the [2-(2,6-dimethylphenoxy)acetyl]amino at the P2′ subsite, and the dodecahydroisoquinoline ring at the P1′ subsite are three major factors affecting the binding affinity of the ligand with the PR.

We speculate that inhibitors with a dodecahydroisoquinoline ring at the P1′ subsite, a [2-(2,6-dimethylphenoxy)acetyl] amino group at the P2′ subsite, and an N2 atom at the P2 subsite will not only favor binding of the ligand with the subtype AE HIV-1 PR but will also have little effect on the V82F mutation.

Acknowledgments We are grateful for support from the Teaching and Research Award Program for Outstanding Young Teachers in High Education Institutions of Ministry of Education of the People's Republic of China, and from the Liaoning Science and Technology Foundation (No. 2005226008).

References

1. Wlodawer A (2002) Annu Rev Med 53:595. doi:10.1146/annurev.med.53.052901.131947
2. Hellen CU, Krausslich HG, Wimmer E (1989) Biochemistry 28:9881. doi:10.1021/bi00452a001
3. Kohl NE, Emini EA, Schleif WA, Davis LJ, Heimbach JC, Dixon RA, Scolnick EM, Sigal IS (1988) Proc Natl Acad Sci USA 85:4686. doi:10.1073/pnas.85.13.4686
4. Swanstrom R, Erona J (2000) Pharmacol Ther 86:145. doi:10.1016/S0163-7258(00)00037-1
5. Craig JC, Duncan IB, Hockley D, Grief C, Roberts NA, Mills JS (1991) Antiviral Res 16:295. doi:10.1016/0166-3542(91)90045-S
6. Vacca JP, Dorsey BD, Schleif WA, Leven RB, McDaniel SL, Darke PL, Zugay J, Quintero JC, Blahy OM, Roth E, Sardana VV, Schlabach AJ, Graham PI, Condra JH, Gotlib L, Holloway MK, Lin J, Chen L-W, Vastag K, Ostvic D, Anderson PS, Emini EA, Huff JR (1994) Proc Natl Acad Sci USA 91:4096. doi:10.1073/pnas.91.9.4096
7. Livington DJ, Pazhanisamy S, Porter DJ, Partaledis JA, Tung RD, Painter GR (1995) J Infect Dis 172:238
8. Patick AK, Mo H, Markowitz M, Appelt K, Wu B, Musick L, Kalish V, Kaldor S, Reich S, Ho D, Webber S (1996) Antimicrob Agents Chemother 40:292 Erratum, p 1575
9. Carrillo A, Stewart KD, Sham HL, Norbeck DW, Kohlbrenner WE, Leonard JM, Kempf DJ, Molla AJ (1998) J Virol 72:7532
10. Robinson BS, Riccardi KA, Gong YF, Guo Q, Stock DA, Blair WS, Terry BJ, Deminie CA, Djang F, Colonno RJ, Lin PF (2000) Antimicrob Agents Chemother 44:2093. doi:10.1128/AAC.44.8.2093-2099.2000
11. Larder BA, Hertogs K, Bloor S, van den Eynde C, DeCian W, Wang Y, Freimuth WW, Tarpley G (2000) AIDS 14:1943. doi:10.1097/00002030-200009080-00009
12. Koh Y, Nakata H, Maeda K, Ogata H, Bilcer G, Devasamudram T, Kincaid JF, Boross P, Wang YF, Tie Y, Volarath P, Gaddis L, Harrison RW, Weber IT, Ghosh AK, Mitsuya H (2003) Antimicrob Agents Chemother 47:3123. doi:10.1128/AAC.47.10.3123-3129.2003
13. Wainberg MA (2004) AIDS 18(Suppl 3):S63. doi:10.1097/00002030-200406003-00012
14. Wlodawer A, Miller M, Jaskolski M, Sathyanarayana BK, Baldwin E, Weber IT, Selk LM, Clawson L, Schneider J, Kent SBH (1989) Science 245:616. doi:10.1126/science.2548279
15. Kempf DJ, Marsh KC, Denissen JF, McDonald E, Vasavanonda S, Flentge CA, Green BE, Fino L, Park CH, Kong XP (1995) Proc Natl Acad Sci USA 92:2484. doi:10.1073/pnas.92.7.2484
16. Prabu-Jeyabalan M, Nalivaika E, Schiffer CA (2002) Structure 10:369. doi:10.1016/S0969-2126(02)00720-7
17. Nam KY, Chang BH, Han CK, Ahn SK, No KT (2003) Bull Korean Chem Soc 24:817
18. Wittayanarakul K, Hannongbua S, Feig M (2007) J Comput Chem 29:673. doi:10.1002/jcc.20821
19. Zoete V, Michielin O, Karplus M (2002) J Mol Biol 315:21. doi:10.1006/jmbi.2001.5173
20. Seibold SA, Cukier RI (2007) Proteins 69:551. doi:10.1002/prot.21535
21. Lauria A, Ippolito M, Almerico AM (2007) J Mol Model 13:1151. doi:10.1007/s00894-007-0242-3
22. Barbaro G, Scozzafava A, Mastrolorenzo A, Supuran CT (2005) Curr Pharm Des 11:1805. doi:10.2174/1381612053764869
23. Ohtaka H, Freire E (2005) Prog Biophys Mol Biol 88:193. doi:10.1016/j.pbiomolbio.2004.07.005
24. Ghosh AK, Dawson ZL, Mitsuya H (2007) Bioorg Med Chem 15:7576. doi:10.1016/j.bmc.2007.09.010
25. Surleraux DLNG, de Kock HA, Verschueren WG, Pille GME (2005) J Med Chem 48:1965. doi:10.1021/jm049454n
26. Surleraux DLNG, Tahri A, Verschueren WG, Pille GME, de Kock HA, Jonckers THM, Peeters A, Meyer SD, Azijn H, Pauwels R, de Bethune MP, King NM, Jeyabalan MP, Schiffer CA, Wigerinck PBTP (2005) J Med Chem 48:1813. doi:10.1021/jm049560p
27. Rick SW, Topol IA, Erickson JW, Burt SK (1998) Protein Sci 7:1750
28. Piana S, Carloni P, Rothlisberger U (2002) Protein Sci 11:2393. doi:10.1110/ps.0206702
29. Clemente JC, Hermrajani R, Blum LE, Goodenow MM, Dunn BM (2003) Biochemistry 42:15029. doi:10.1021/bi035701y

30. Perryman AL, Lin JH, McCammon JA (2003) Protein Sci 13:1108. doi:10.1110/ps.03468904
31. Ode H, Ota M, Neya S, Hata M, Sugiura W, Hoshino T (2005) J Phys Chem B 109:565. doi:10.1021/jp046860+
32. Wittayanarakul K, Aruksakunwong O, Saen-oon S, Chantratita W, Parasuk V, Sompornpisut P, Hannongbua S (2005) Biophys J 88:867. doi:10.1529/biophysj.104.046110
33. Chen RX, Quinones-Mateu ME, Mansky LM (2004) Curr Pharm Des 10:4065. doi:10.2174/1381612043382404
34. Clavel F, Hance AJ (2004) N Engl J Med 350:1023. doi:10.1056/NEJM2ra025195
35. D'Aquila RT, Schapiro JM, Brun-Vezinet F, Clotet B, Conway B, Demeter LM, Grant RM, Johnson VA, Kuritzkes DR, Loveday C, Shafer RW, Richman DD (2002) Top HIV Med 10:21
36. Shuman CF, Markgren PO, Hämäläinen M, Danielson UH (2003) Antiviral Res 58:235. doi:10.1016/S0166-3542(03)00002-0
37. Ghosh AK, Chapsal BD, Weber IT, Mitsuya H (2008) Acc Chem Res 41:78. doi:10.1021/ar7001232
38. Kovalevsky AY, Tie YF, Liu FL, Boross PI, Wang YF, Leshchenko S, Ghosh AK, Harrison RW, Weber IT (2006) J Med Chem 49:1379. doi:10.1021/jm050943c
39. Liu FL, Boross PI, Wang YF, Tozser J, Louis JM, Harrison RW, Weber IT (2005) J Mol Biol 354:78940. doi:10.1016/j.jmb.2005.09.095
40. Ohtaka H, Campoy AV, Xie D, Freire E (2002) Protein Sci 11:1908. doi:10.1110/ps.0206402
41. Liu FL, Kovalevsky AY, Louis JM, Boross PI, Wang YF, Harrison RW, Weber IT (2006) J Mol Biol 358:1191. doi:10.1016/j.jmb.2006.02.076
42. Perrin V, Mammano F (2003) J Virol 77:10172. doi:10.1128/JVI.77.18.10172-10175.2003
43. Kantor R, Fessel WJ, Zolopa AR, Israelski D, Shulman N, Montoya JG, Harbour M, Schapiro JM, Shafer RW (2002) Antimicrob Agents Chemother 46:1086. doi:10.1128/AAC.46.4.1086-1092.2002
44. Wu TD, Schiffer CA, Gonzales MJ, Taylor J, Kantor R, Chou S, Israelski D, Zolopa AR, Fessel WJ, Shafer RW (2003) J Virol 77:4836. doi:10.1128/JVI.77.8.4836-4847.2003
45. Jacobsen H, Yasargil K, Winslow DL, Craig JC, Krohn A, Duncan IB, Mous J (1995) J Virol 206:527. doi:10.1016/S0042-6822(95)80069-7
46. Velazquez-Campoy A, Vega S, Freire E (2002) Biochemistry 41:8613. doi:10.1021/bi020160i
47. Cornelissen M, van den Burg R, Zorgdrager F, Lukashov V, Goudsmit J (1997) J Virol 71:6348
48. Pieniazek D, Rayfield M, Hu DJ, Nkengasong J, Wiktor SZ, Downing R, Biryahwaho B, Mastro T, Tanuri A, Soriano V, Lal R, Dondero T (2000) AIDS 14:1489. doi:10.1097/00002030-200007280-00004
49. Grossman Z, Vardinon N, Chemtob D, Alkan ML, Bentwich Z, Burke M, Gottesman G, Istomin V, Levi I, Maayan S, Shahar E, Schapiro JM (2001) AIDS 15:1453. doi:10.1097/00002030-200108170-00001
50. Vergne L, Peeters M, Mpoudi-Ngole E, Bourgeois A, Liegeois F, Toure-Kane C, Mboup S, Mulanga-Kabeya C, Saman E, Jourdan J, Reynes J, Delaporte E (2000) J Clin Microbiol 38:3919
51. Burke DS, McCutchan FE (1996) AIDS: biology, diagnostics, treatment and prevention, 4th edn. Lippincott–Raven, New York
52. Montano MA, Novitsky VA, Blackard JT, Cho NL, Katzenstein DA, Essex M (1997) J Virol 71:8657
53. Spira S, Wainberg MA, Loemba H, Turner D, Brenner BG (2003) J Antimicrob Chemother 51:229. doi:10.1093/jac/dkg079
54. Aruksakunwong O, Wolschann P, Hannongbua S, Sompornpisut P (2006) J Chem Inf Model 46:2085. doi:10.1021/ci060090c
55. Hou TJ, Yu R (2007) J Med Chem 50:1177. doi:10.1021/jm0609162
56. Clemente JC, Coman RM, Thiaville MM, Janka LK, Jeung JA, Nukoolkarn S, Govindasamy L, Agbandje-McKenna M, McKenna R, Leelamanit W, Goodenow MM, Dunn BM (2006) Biochemistry 45:5468. doi:10.1021/bi051886s
57. Stoll V, Qin W, Stewart KD, Jakob C, Park C, Walter K, Simmer RL, Helfrich R, Bussiere D, Kao J, Kempf D, Sham HL, Norbeck DW (2002) Bioorg Med Chem 10:2803. doi:10.1016/S0968-0896(02)00051-2
58. Kaldor SW, Kalish VJ, Davies JF, Shetty BV, Fritz JE, Appelt K, Burgess JA, Campanale KM, Chirgadze NY, Clawson DK, Dressman BA, Hatch SD, Khalil DA, Kosa MB, Lubbehusen PP, Muesing MA, Patick AK, Reich SH, Su KS, Tatlock JH (1997) J Med Chem 40:3979. doi:10.1021/jm9704098
59. Case DA, Darden TA, Cheatham TEIII, Simmerling CL, Wang J, Duke RE, Luo R, Merz KM, Pearlman DA, Crowley M, Walker RC, Zhang W, Wang B, Hayik S, Roitberg A, Seabra G, Wong KF, Paesani F, Wu X, Brozell S, Tsui V, Gohlke H, Yang L, Tan C, Mongan J, Hornak V, Cui G, Beroza P, Mathews DH, Schafmeister C, Ross WS, Kollman PA (2006) AMBER 9. University of California, San Francisco
60. Frisch J, Trucks GW, Schlegel HB, Scuseria GE, Robb MA, Cheeseman JR, Montgomery JA Jr, Vreven T, Kudin KN, Burant JC, Millam JM, Iyengar SS, Tomasi J, Barone V, Mennucci B, Cossi M, Scalmani G, Rega N, Petersson GA, Nakatsuji H, Hada M, Ehara M, Toyota K, Fukuda R, Hasegawa J, Ishida M, Nakajima T, Honda Y, Kitao O, Nakai H, Klene M, Li X, Knox JE, Hratchian HP, Cross JB, Adamo C, Jaramillo J, Gomperts R, Stratmann RE, Yazyev O, Austin AJ, Cammi R, Pomelli C, Ochterski JW, Ayala PY, Morokuma K, Voth GA, Salvador P, Dannenberg JJ, Zakrzewski VG, Dapprich S, Daniels AD, Strain MC, Farkas O, Malick DK, Rabuck AD, Raghavachari K, Foresman JB, Ortiz JV, Cui Q, Baboul AG, Clifford S, Cioslowski J, Stefanov BB, Liu G, Liashenko A, Piskorz P, Komaromi I, Martin RL, Fox DJ, Keith T, Al-Laham MA, Peng CY, Nanayakkara A, Challacombe M, Gill PMW, Johnson B, Chen W, Wong MW, Gonzalez C, Pople JA (2003) GAUSSIAN 03, Revision B.05. Gaussian Inc., Pittsburg
61. Cieplak P, Cornell WD, Bayly C, Kollman PA (1995) J Comput Chem 16:1357. doi:10.1002/jcc.540161106
62. Wang J, Cieplak P, Kollman PA (2000) J Comput Chem 21:1049. doi:10.1002/1096-987X(200009)21:12<1049::AID-JCC3>3.0.CO;2-F
63. Dolinsky TJ, Nielsen JE, McCammon JA, Baker NA (2004) Nucleic Acids Res 32:W665. doi:10.1093/nar/gkh381
64. Ryckaert JP, Ciccotti G, Berendsen HJC (1977) J Comput Phys 23:327. doi:10.1016/0021-9991(77)90098-5
65. Darden T, York D, Pedersen L (1993) J Chem Phys 98:10089. doi:10.1063/1.464397
66. Wang JM, Hou TJ, Xu XJ (2006) Curr Comput-Aided Drug Des 2:287. doi:10.2174/157340906778226454
67. Rocchia W, Alexov E, Honig B (2001) J Phys Chem B 105:6507. doi:10.1021/jp010454y
68. Stoica I, Sadiq SK, Coveney PV (2008) J Am Chem Soc 130:2639. doi:10.1021/ja0779250
69. Lee B, Richards FM (1971) J Mol Biol 55:379. doi:10.1016/0022-2836(71)90324-X
70. Connolly ML (1983) J Appl Cryst 16:548. doi:10.1107/S0021889883010985
71. Ode H, Neya S, Hata M, Sugiura W, Hoshino T (2006) J Am Chem Soc 128:7887. doi:10.1021/ja060682b
72. Kuhn LA, Siani MA, Pique ME, Fisher CL, Getzoff ED, Tainer JA (1992) J Mol Biol 228:13. doi:10.1016/0022-2836(92)90487-5
73. Chothia C (1976) J Mol Biol 105:1. doi:10.1016/0022-2836(76)90191-1
74. Nozaki Y, Tanford C (1971) J Biol Chem 7:2211
75. Strisovsky K, Tessmer U, Langner J, Konvalinka J, Kräusslich HG (2000) Protein Sci 9:1631